

Beyond the Bowen-York extrinsic curvature for spinning black holes

Mark Hannam, Sascha Husa, Bernd Brügmann, José A. González, Ulrich Sperhake

Theoretical Physics Institute, University of Jena, 07743 Jena, Germany

Abstract. It is well-known that Bowen-York initial data contain spurious radiation. Although this “junk” radiation has been seen to be small for non-spinning black-hole binaries in circular orbit, its magnitude increases when the black holes are given spin. It is possible to reduce the spurious radiation by applying the puncture approach to multiple Kerr black holes, as we demonstrate for examples of head-on collisions of equal-mass black-hole binaries.

PACS numbers: 04.20.Ex, 04.25.Dm, 04.30.Db, 95.30.Sf

1. Introduction

Fully general relativistic numerical simulations of black-hole binaries have one remarkable advantage over all analytic approximation techniques (perturbation theory, close-limit analyses and post-Newtonian calculations): given the correct initial data, simulations take into account *all* of the physics in the problem. One may be limited by computer resources and the accuracy of a given numerical technique, but in principle no physics has been oversimplified or overlooked in the calculation.

We are left with one qualifier: the initial data must be physically correct. Producing good initial data involves finding physically realistic solutions of the constraint equations of general relativity, and providing the appropriate physical parameters for those solutions. The most commonly used initial data for recent evolutions of black-hole binaries have been puncture data based on the Bowen-York extrinsic curvature [1, 2] — of the eight codes reported to have successfully performed long-term evolutions of several orbits [3, 4, 5, 6, 7, 8, 9, 10], six use Bowen-York puncture data.

One problem with these data is that they contain unwanted spurious gravitational radiation. For example, a spinning Bowen-York black hole is a Kerr black hole plus a Brill wave [11]. In evolutions of black-hole binaries the spurious radiation can be recognized as an initial “bump” in the extracted gravitational waveform. It is interesting that this bump also appears in evolutions performed using data produced within the conformal thin sandwich (CTS) formulation of the initial-value equations [12], and is even present in evolutions that start with boosted scalar fields that later collapse to form black holes [3].

In Bowen-York data, we know that the initial burst of spurious radiation is partly due to the Bowen-York form of the conformal extrinsic curvature. The magnitude of the spurious radiation grows with both the linear momentum and spin assigned to each black hole. We may therefore worry that the “junk” radiation will significantly perturb the desired orbit of the binary. For unequal-mass binaries this worry is justified: one sees that the spurious radiation imparts a significant initial “kick” to the black holes [13].

In this paper we describe a technique to reduce this spurious radiation for spinning black holes, using a superposition of Kerr solutions in puncture form. This technique is similar in spirit to the superposition of Kerr-Schild black holes [14, 15, 16, 17], but with the advantage that it easily fits into the puncture framework that has proved so useful for recent black-hole simulations. In the following sections we will summarize the construction of black-hole initial data, outline the new method to produce superposed Kerr punctures, and present first results of head-on collisions of Kerr punctures, which demonstrate that the junk radiation has indeed been reduced.

2. Decomposition of the initial-value equations

We start with the standard 3+1 decomposition [18], whereby the Einstein equations are separated into initial-value and evolution equations. An additional conformal decomposition results in initial-value equations for which there are free data, which must be specified, and constrained data that must satisfy the conformally decomposed constraint equations.

The Bowen-York solution to the momentum constraint was originally found in the context of the conformal transverse-traceless (CTT) decomposition [1]. This solution has the great advantage that the linear momenta and spins of multiple black holes can be easily specified; the global properties of the data are free parameters. On the other hand, the choices of the free data in the CTT decomposition necessary to obtain the Bowen-York solution were made for convenience, and without strong physical motivation. It has been argued [19] that better physically motivated choices can be made for the free data in the more recent conformal thin-sandwich decomposition [20], and that these may lead to more astrophysically realistic initial data.

However, as we will see below, the most obvious physical choices of the free data in the CTS decomposition are the *same* as those used to construct the Bowen-York solution, and that the difference between the two constructions may largely be a difference in coordinate choice.

In the 3+1 decomposition of Einstein's equations, the constraints are coupled elliptic equations for the spatial metric γ_{ij} and extrinsic curvature K_{ij} on one time slice:

$$\nabla_j (K^{ij} - \gamma^{ij} K) = 0, \quad (1)$$

$$R + K^2 - K_{ij} K^{ij} = 0, \quad (2)$$

where ∇_i is the covariant derivative compatible with the spatial metric γ_{ij} . The constraint equations can be further decomposed using a conformal transformation. The spatial metric γ_{ij} is related to a background metric $\tilde{\gamma}_{ij}$ via a conformal factor ψ ,

$$\gamma_{ij} = \psi^4 \tilde{\gamma}_{ij}. \quad (3)$$

The extrinsic curvature is also decomposed. In the conformal thin-sandwich decomposition [20], we define $\tilde{u}_{ij} = \partial_t \tilde{\gamma}_{ij}$. The extrinsic curvature is split into its trace and tracefree parts, and can be written in terms of the lapse function N and the shift vector β^i ,

$$K_{ij} = \psi^{-2} \tilde{A}_{ij} + \psi^4 \tilde{\gamma}_{ij} K \quad (4)$$

$$= \psi^{-2} \left[\frac{1}{2N} \left((\tilde{\mathbb{L}}\beta)_{ij} - \tilde{u}_{ij} \right) \right] + \psi^4 \tilde{\gamma}_{ij} K \quad (5)$$

$$= \frac{1}{2N} [(\mathbb{L}\beta)_{ij} - u_{ij}] + \gamma_{ij} K. \quad (6)$$

The conformal weights of the variables in these equations are

$$N = \psi^6 \tilde{N}, \quad (7)$$

$$\beta^i = \tilde{\beta}^i, \quad (8)$$

$$u_{ij} = \psi^4 \tilde{u}_{ij}, \quad (9)$$

$$K = \tilde{K}, \quad (10)$$

and we are free to choose the function \tilde{N} .

Let us now make the standard “quasi-equilibrium” choices of the free data [19] that have been used when numerically producing CTS data [21, 22, 19, 23, 24, 25, 26, 27, 28, 29, 30]: conformal flatness, $\tilde{\gamma}_{ij} = f_{ij}$, maximal slicing, $K = 0$, and initial stationarity of the conformal metric, $\tilde{u}_{ij} = 0$. If, in addition, we choose that $\tilde{N} = 1/2$, the Hamiltonian and momentum constraints reduce to the same form as in the conformal transverse-traceless decomposition:

$$\tilde{\nabla}_j \tilde{A}^{ij} = 0 \quad (11)$$

$$\tilde{\nabla}^2 \psi = -\frac{1}{8} \psi^7 \tilde{A}_{ij} \tilde{A}^{ij}. \quad (12)$$

The Bowen-York extrinsic curvature is a solution to this form of the momentum constraint, and we see that Bowen-York data satisfies all of the quasi-equilibrium requirements of CTS data.

The one extra ingredient in the standard construction of CTS data is another quasi-equilibrium requirement, $\partial_t K = 0$, which yields an elliptic equation for \tilde{N} . This “extended CTS” system can be shown to admit non-unique solutions in some cases [31, 32, 33], but these problems have not prevented the construction of initial data for black-hole binaries. The extra requirement $\partial_t K = 0$ will make some change to the physics of the system, but it is not clear what that change will be, and it is certainly unclear whether the resulting data will be any more “astrophysically realistic” than Bowen-York data. Initial-data studies that calculate the innermost stable circular orbit (ISCO) for standard CTS data [22, 25, 28, 29] find that its location better matches post-Newtonian predictions than for Bowen-York data [34, 35]. However, recent numerical simulations of inspiralling black holes have cast doubt on how much sense it makes to discuss an ISCO for comparable-mass black holes, so it is not clear how much weight to give to the conclusions from these initial-data studies. One thing is certainly clear from dynamic numerical simulations: moving from Bowen-York to CTS data does not noticeably improve the spurious radiation content of the initial data. (Compare, for example, Figure 2 in [36] with Figure 2 in [12].)

In the following, we will choose a function \tilde{N} that is convenient for the numerical solution of the constraints. The solutions of the conformal thin-sandwich initial-value equations, together with the choice of \tilde{N} , provide us with a lapse $N = \psi^6 \tilde{N}$ and a shift vector β^i , but these are not necessarily ideal for dynamical evolutions. In particular, our choice for \tilde{N} will imply a lapse function that blows up at the punctures, and would produce slices that hit the singularities in an infinitely short time! For evolutions we instead make the standard choices $N = 1$ and $\beta^i = 0$ on the initial slice.

3. Puncture approach

Given the Bowen-York solution of the momentum constraint, we are left to solve the Hamiltonian constraint to complete the specification of the initial data. It is convenient to choose the ansatz [2],

$$\psi = 1 + \sum_i \frac{m_i}{2r_i} + u, \quad (13)$$

where the m_i parametrize the masses of the black holes, and the r_i are the coordinate distances to each ‘‘puncture’’. The Hamiltonian constraint now reduces to an elliptic equation for the function u . In this work, the Hamiltonian constraint is solved using the fixed-mesh-refinement multigrid solver in the BAM code [9].

There are many advantages to this approach. The n black holes are constructed with a topology that consists of $n+1$ asymptotically flat ends connected by n wormholes, and the slice, by construction, avoids the singularities. As a result, the initial-value equations can be solved on all of R^3 , without any need to excise a region around each black hole. A second advantage is that it is possible to stably evolve these data, and although connection with the extra asymptotically flat ends may be lost with particular gauge choices [37], the slices remain singularity avoiding, and one need never resort to excision techniques.

When constructing Kerr-like punctures, we will also have to numerically solve the momentum constraint. Although the conformal extrinsic curvature will diverge at the punctures, we can ensure that the elliptic solver deals only with non-divergent functions by a suitable choice of the conformal lapse, \tilde{N} .

4. Head-on collisions with spinning punctures

Let us first consider the spurious radiation content of spinning Bowen-York punctures. As a simple illustration, we will present evolutions of head-on collisions of equal-mass black holes with their spins directed away from each other. In this way, we expect the final black hole to be non-spinning, i.e., a Schwarzschild black hole.

Evolutions are performed with the BAM code [9], using the BSSN formulation of the evolution equations [38, 39]. The lapse function and shift vector are initially $N = 1$ and $\beta^i = 0$, and are evolved using the 1+log [40] and $\tilde{\Gamma}$ -driver [41] slicing conditions.

Figure 1 shows the results from runs that started with punctures of masses $M_1 = M_2 = 0.5$ placed at $z = \pm 4M$ (where $M = M_1 + M_2$), and given spins $|S_z| = 0, 0.6, 0.8, 0.9M^2$, such that the spins were directed away from the origin. The figure shows the $(l = 2, m = 0)$ mode of the real part of $r\Psi_4$, extracted at $r = 20M$. (See [9] for a description of the wave-extraction algorithm in the BAM code.)

The gravitational radiation from the merger is clearly visible after about $60M$ of evolution. Prior to that, some spurious radiation can be seen even when $S_z = 0$. This is presumably due to some unphysical component to the Brill-Lindquist solution when the black holes are close. We do not expect the Brill-Lindquist solution to be physically

realistic unless the black holes are infinitely far apart, and indeed the spurious radiation decreases as the black holes are placed further apart, as is clearly seen in [7]. (See also [42] for a post-Newtonian extension of Brill-Lindquist data.)

As spin is added, extra spurious initial radiation is seen. The extra spurious radiation has roughly the quasinormal mode frequency of each of the individual black holes. For the case where $|S_z| = 0.9M^2$, the initial “junk” radiation is of comparable magnitude to the radiation from the black holes’ merger. (We should point out that this for

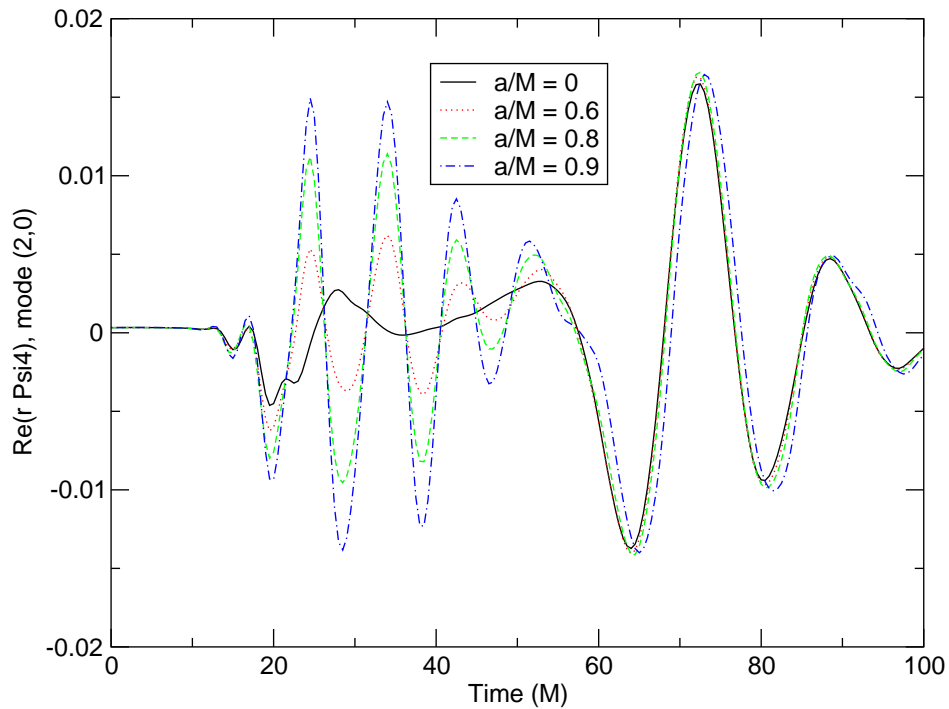


Figure 1. The spurious gravitational radiation from the head-on collision of equal-mass ($M_1 = M_2 = 0.5$) Bowen-York punctures. The punctures are placed at $z = \pm 4M$ and given spins $a/M_i = |S_z|/M_i^2 = 0, 0.6, 0.8, 0.9$, such that the spins are directed away from the origin.

5. Kerr-like data for black-hole binaries

Now we wish to reduce the initial radiation content for spinning punctures. Motivated by Dain’s work in [44, 45], we extend work done by Krivan and Price in axisymmetry [46]. We start by writing the Kerr metric for a black hole with mass m and angular momentum a/m in quasi-isotropic coordinates [11, 44]:

$$\tilde{\gamma}_{ij} = \delta_{ij} + a^2 h(m, a, r, \theta) v_{ij}, \quad (14)$$

$$v_{ij} = \{(y^2, -xy, 0), (-xy, x^2, 0), (0, 0, 0)\}, \quad (15)$$

$$\psi = 1 + \frac{\sqrt{m^2 - a^2}}{2r} + u_{\text{Kerr}} \quad (16)$$

$$\tilde{A}_{ij} = \tilde{A}_{ij}^{\text{Kerr}}. \quad (17)$$

The analytic functional forms of $\tilde{A}_{ij}^{\text{Kerr}}$ and u_{Kerr} are given in [11] and [46].

This form of the metric, which appears in [44], can be generalized to two black holes by superposition:

$$\tilde{\gamma}_{ij} = \delta_{ij} + a_1^2 h_1 v_{ij}^1 + a_2^2 h_2 v_{ij}^2, \quad (18)$$

$$\tilde{A}_{ij} = \tilde{A}_{ij}^{K1} + \tilde{A}_{ij}^{K2} + \frac{1}{2\tilde{N}}(\mathbb{L}\beta)_{ij}. \quad (19)$$

The background metric is a piece of the free data, so a straightforward superposition is acceptable. The conformal extrinsic curvature must satisfy the momentum constraint, so we consider it as a superposition of the conformal extrinsic curvatures from two single Kerr punctures, \tilde{A}_{ij}^{K1} and \tilde{A}_{ij}^{K2} , plus a correction that we must solve for numerically, and which we write in a form motivated by (6). We continue to make the choice of maximal slicing, $K = 0$. This construction is similar in spirit to that applied to Kerr-Schild data by Matzner, Huq and Shoemaker [14]. Another related work is [47], where the authors adopted the Kerr form of the extrinsic curvature, but retained conformal flatness.

The constraints now take the form

$$\tilde{\nabla}^2 \psi = -\frac{1}{8}\psi^{-7}\tilde{A}_{ij}\tilde{A}^{ij} + \frac{1}{8}\psi\tilde{R}, \quad (20)$$

$$\tilde{\Delta}_{\mathbb{L}}\beta^i - (\tilde{\mathbb{L}}\beta)^{ij}\tilde{\nabla}_j \ln \tilde{N} = -2\tilde{N}\tilde{\nabla}_j(\tilde{A}_{K1}^{ij} + \tilde{A}_{K2}^{ij}). \quad (21)$$

Note that in the Kerr case the conformal Ricci scalar \tilde{R} is non-zero and diverges at the punctures. However, the Laplacian of ψ with respect to the background metric (18) diverges in the same way as $\psi\tilde{R}$, and the final right-hand side of the Hamiltonian constraint is finite and sufficiently well-behaved that the code is able to generate numerical solutions.

To solve the Hamiltonian constraint, we write the conformal factor in the standard puncture form,

$$\psi = 1 + \sum_i^n \frac{\sqrt{m_i^2 - a_i^2}}{2r_i} + u \equiv \psi_0 + u, \quad (22)$$

where $\sqrt{m_i^2 - a_i^2}$ is motivated by the form of ψ for the Kerr solution in quasi-isotropic coordinates, Eqn. (16).

In order to solve the momentum constraint numerically, we make a new choice for the conformal lapse,

$$\tilde{N} = \psi_0^{-3} \quad (23)$$

The reason for this choice is that the $\tilde{A}_{ij}^{K1,2}$ diverge at the punctures as r^3 , but introducing a factor of $\psi^{-3} \sim r^3$ makes the right-hand side of (21) finite at the punctures.

The constraints were solved using the multigrid solver in the BAM code [9], and the initial data (γ_{ij}, K_{ij}) reconstructed using (3) - (10).

Figure 2 shows the results of evolving configurations equivalent to those considered in Figure 1 for head-on collisions of spinning Bowen-York punctures. We see that the

spurious radiation from the initial data deviates much less from that in the non-spinning Brill-Lindquist case. There are some high-frequency components to the junk radiation, but these may be due to the low tolerance used in the elliptic solver; this requires more analytic and numerical study. The main result is clear: the superposed Kerr punctures contain

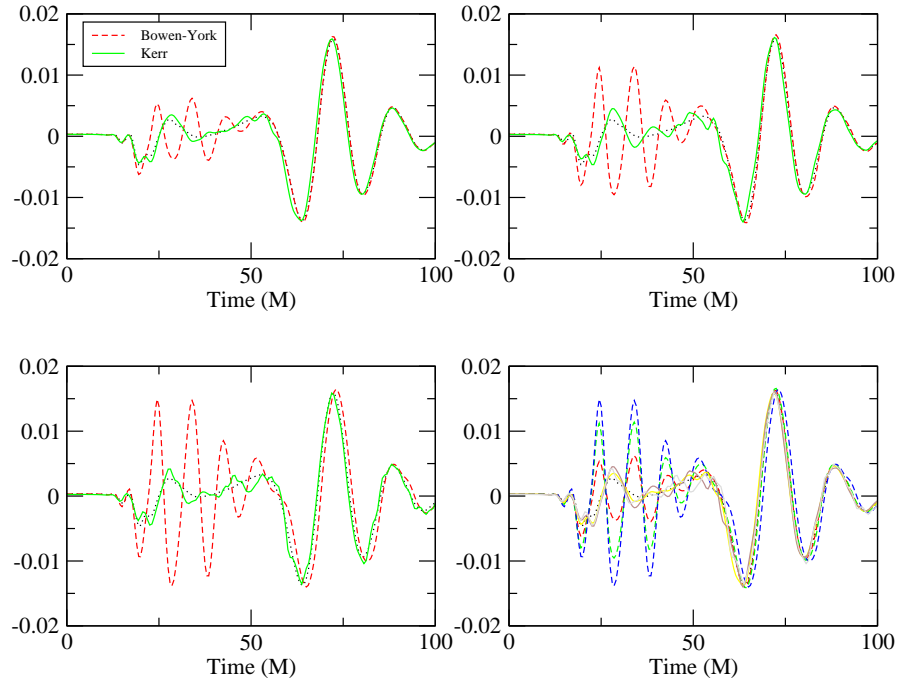


Figure 2. Spurious radiation from head-on collisions of spinning Bowen-York and Kerr-like punctures, for spins of $a/M = 0.6$ (top-left), 0.8 (top-right), 0.9 (lower-left), and all three (lower-right). The quantity shown in each plot is the $(l = 2, m = 0)$ mode of $r\Psi_4$ extracted at $20M$. In each plot the dotted black line corresponds to the radiation from a collision of nonspinning (Brill-Lindquist) punctures. In the top-left, top-right and lower-left plots, the dashed line shows the radiation from Bowen-York punctures, as also shown in Figure 1, and the solid line shows the radiation from Kerr-like punctures. The lower-right plot allows a comparison between the three choices of spin.

6. Conclusions

We have presented a method to construct initial data for two Kerr-like black holes in the puncture framework. This construction is based on the form of the Kerr metric in quasi-isotropic coordinates [11], and following the suggestions outlined in [44, 45] extends the work in axisymmetry of [46].

For the simple test case of a head-on collision of two black holes, we have demonstrated that the new initial data contain significantly less spurious gravitational radiation than their popular Bowen-York counterparts.

The results here serve as an illustration of the potential of this method. In

future work we will explore its effectiveness in more general configurations, and extend the construction to spinning black holes that also possess linear momentum. Such a construction would be necessary to make these data a feasible alternative to Bowen-York data for simulations of black-hole binary inspiral.

Acknowledgments

This work was supported in part by DFG grant SFB/Transregio 7 “Gravitational Wave Astronomy”. Computations where performed at HLRS (Stuttgart) and LRZ (Munich).

References

- [1] Bowen J M and York J W 1980 *Phys. Rev. D* **21**(8) 2047–2056
- [2] Brandt S and Brügmann B 1997 *Phys. Rev. Lett.* **78**(19) 3606–3609 (*Preprint* [gr-qc/9703066](#))
- [3] Pretorius F 2005 *Phys. Rev. Lett.* **95** 121101 (*Preprint* [gr-qc/0507014](#))
- [4] Campanelli M, Lousto C O, Marronetti P and Zlochower Y 2006 *Phys. Rev. Letter* **96** 111101
- [5] Baker J G, Centrella J, Choi D I, Koppitz M and van Meter J 2006 *Phys. Rev. Lett.* **96** 111102
- [6] Herrmann F, Shoemaker D and Laguna P 2006 (*Preprint* [gr-qc/0601026](#))
- [7] Sperhake U 2006 (*Preprint* [gr-qc/0606079](#))
- [8] Scheel M A *et al.* 2006 *Phys. Rev.* **D74** 104006
- [9] Brügmann B, González J A, Hannam M, Husa S, Sperhake U and Tichy W 2006 (*Preprint* [gr-qc/0610128](#))
- [10] Pollney D July 2006 Presented at the *New Frontiers in Numerical Relativity* meeting, Golm
- [11] Brandt S and Seidel E 1996 *Phys. Rev. D* **54**(2) 1403–1416
- [12] Buonanno A, Cook G and Pretorius F 2006 (*Preprint* [gr-qc/0610122](#))
- [13] Gonzalez J A, Sperhake U, Bruegmann B, Hannam M and Husa S 2006 (*Preprint* [gr-qc/0610154](#))
- [14] Matzner R A, Huq M F and Shoemaker D 1999 *Phys. Rev. D* **59** 024015
- [15] Marronetti P, Huq M F, Laguna P, Lehner L, Matzner R A and Shoemaker D 2000 *Phys. Rev. D* **62** 024017
- [16] Marronetti P and Matzner R A 2000 *Phys. Rev. Lett.* **85** 5500–5503
- [17] Bonning E, Marronetti P, Neilsen D and Matzner R 2003 *Phys. Rev. D* **68** 044019
- [18] York J W 1979 in L L Smarr, ed, *Sources of gravitational radiation* (Cambridge, UK: Cambridge University Press) pp 83–126 ISBN 0-521-22778-X
- [19] Cook G B 2002 *Phys. Rev. D* **65** 084003
- [20] York J W 1999 *Phys. Rev. Lett.* **82** 1350–1353
- [21] Gourgoulhon E, Grandclément P and Bonazzola S 2002 *Phys. Rev. D* **65** 044020
- [22] Grandclément P, Gourgoulhon E and Bonazzola S 2002 *Phys. Rev. D* **65** 044021
- [23] Pfeiffer H P, Cook G B and Teukolsky S A 2002 *Phys. Rev. D* **66** 024047
- [24] Pfeiffer H P and York J W 2003 *Phys. Rev. D* **67** 044022
- [25] Cook G B and Pfeiffer H P 2004 *Phys. Rev. D* **70**
- [26] Ansorg M 2005 *Phys. Rev. D* **72** 024018
- [27] Hannam M D and Cook G B 2005 *Phys. Rev. D* **71** 084023
- [28] Hannam M D 2005 *Phys. Rev. D* **72** 044025
- [29] Caudill M, Cook G B, Grigsby J D and Pfeiffer H P 2006 *Phys. Rev. D* **74** 064011
- [30] Jaramillo J L, Ansorg M and Limousin F 2006 (*Preprint* [gr-qc/0610006](#))
- [31] Pfeiffer H P and York J W 2005 *Phys. Rev. Lett.* **95** 091101
- [32] Baumgarte T W, Murchadha N O and Pfeiffer H P 2006 (*Preprint* [gr-qc/0610120](#))
- [33] Walsh D M 2006 (*Preprint* [gr-qc/0610129](#))
- [34] Cook G B 1994 *Phys. Rev. D* **50**(8) 5025–5032

- [35] Baumgarte T W 2000 *Phys. Rev. D* **62** 024018
- [36] Baker J G, Centrella J, Choi D I, Koppitz M and van Meter J 2006 *Phys. Rev. D* **73** 104002
- [37] Hannam M, Husa S, Pollney D, Brügmann B and Ó Murchadha N 2006 (*Preprint* [gr-qc/0606099](https://arxiv.org/abs/gr-qc/0606099))
- [38] Shibata M and Nakamura T 1995 *Phys. Rev. D* **52** 5428
- [39] Baumgarte T W and Shapiro S L 1999 *Phys. Rev. D* **59** 024007
- [40] Bona C, Massó J, Seidel E and Stela J 1997 *Phys. Rev. D* **56** 3405–3415
- [41] Alcubierre M, Brügmann B, Diener P, Koppitz M, Pollney D, Seidel E and Takahashi R 2003 *Phys. Rev. D* **67** 084023
- [42] Blanchet L 2003 *Phys. Rev. D* **68** 084002
- [43] Campanelli M, Lousto C O and Zlochower Y 2006 *Phys. Rev. D* **74** 041501
- [44] Dain S 2001 *Phys. Rev. Lett.* **87** 121102
- [45] Dain S 2001 *Phys. Rev. D* **64** 124002
- [46] Krivan W and Price R H 1998 *Phys. Rev. D* **58** 104003
- [47] Dain S, Lousto C O and Takahashi R 2002 *Phys. Rev. D* **65** 104038